J|A|C|S
ARTICLES
Published on Web 07/19/2006

Two-Phase Synthesis of Shape-Controlled Colloidal Zirconia Nanocrystals and Their Characterization

Nana Zhao, Daocheng Pan, Wei Nie, and Xiangling Ji*

Contribution from the State Key Laboratory of Polymer Physics and Chemistry, Changchun Institute of Applied Chemistry, Chinese Academy of Sciences, Graduate School of the Chinese Academy of Sciences, 5625 Renmin Street, Changchun 130022, People's Republic of China

Received February 20, 2006; E-mail: xlji@ciac.jl.cn

Abstract: We have developed a two-phase approach for the synthesis of shape-controlled colloidal zirconia nanocrystals, including spherical-, teardrop-, rod-, and rice grain-shaped particles. We found that the key factors for controlling the shape were the reaction time, the nature of the capping agent, and the monomer concentration. We have analyzed the morphologies, crystallinity, optical properties, and structural features of the as-prepared ZrO_2 nanoparticles by using transmission electron microscopy (TEM), high-resolution TEM, X-ray powder diffraction, and UV−vis absorption and fluorescence spectroscopy. The possible nucleation and growth process is also discussed.

Introduction

ZrO_2 is an important ceramic material that has widespread potential applicability in the fields of structural materials, solid-state electrolytes, thermal barrier coatings,[1] electro-optical materials,[2] gas sensing, corrosion resistance, and catalysis.[3] Over the past two decades, several methods have been developed for the preparation of zirconia nanocrystals, including sol−gel,[4−6] hydrothermal/solvothermal,[7,8] thermal decomposition,[9−11] emulsion precipitation,[12] and microwave/sonication-assisted coprecipitation[13] approaches. Another possible general method for preparing zirconia nanocrystals was described recently; it is based on the phase transfer and separation mechanism.[14] Jin et al.[4] synthesized colloidal monodisperse zirconia nanocrystals of 2.9 nm diameter through a nonhydrolytic sol−gel reaction between zirconium(IV) isopropoxide and zirconium(IV) chloride at 340 °C. Noh and co-workers demonstrated the formation of anisotropic ZrO_2 nanocrystalline powders when using a hydrothermal process to perform reactions at temperatures in the range 150−250 °C. Unfortunately, this method is not suitable for producing nanocrystals that possess a narrow size distribution or that can be dispersed completely in certain solvents. The shapes of nanocrystals influence their potential applications. For example, spherical ZrO_2 nanocrystals have been applied as fuel cell electrolytes, oxygen sensors, and gate dielectrics.[7] In contrast, ZrO_2 nanocrystals having anisotropic shapes, such as rod, rice, and leaf morphologies, are expected to be of use in the fabrication of fibers, films, ceramic coatings, and grain-oriented ceramics.[4] Thus, it is desirable to develop a single synthetic approach to provide soluble, shape-controlled ZrO_2 nanocrystals under mild conditions for practical large-scale production. Recently, Pan and Wang developed a two-phase and a two-phase thermal approach for the production of highly luminescent CdS, extremely small CdSe, and CdSe/CdS core/shell quantum dots under relatively mild conditions.[15−17] In addition to these II−VI semiconductors, Pan and co-workers also synthesized luminescent TiO_2 nanocrystals having controllable sizes.[18] In this paper, as a part of our extended work, we report a two-phase thermal route, that is, a two-phase approach combined with an autoclave, for the synthesis of crystalline ZrO_2 nanocrystals having controllable shapes within a narrow size distribution. In this approach, we mixed solutions of zirconium(IV) *n*-propoxide and oleic acid (OA) (or other fatty acid) in toluene and *tert*-butylamine in water and then heated the mixture without stirring. This method exhibits a number of interesting features: (i) The reaction temperature is less than 180 °C; that is, it is much lower than the temperature required for the thermal decomposition process. Indeed, we synthesized nanocrystals even at temperatures below 120 °C. (ii) Nucleation and growth appear to take place continuously without a clear boundary. (iii)

(1) Birkby, I.; Stevens, R. *Key Eng. Mater.* **1996**, *122*, 527−552.
(2) Kourouklis, G. A.; Liarokapis, E. *J. Am. Ceram. Soc.* **1991**, *74*, 520−523.
(3) Murase, Y.; Kato, E. *J. Am. Ceram. Soc.* **1982**, *66*, 196−200.
(4) Joo, J.; Yu, T.; Kim, Y. W.; Park, H. M.; Wu, F.; Zhang, J. Z.; Hyeon, T. *J. Am. Chem. Soc.* **2003**, *125*, 6553−6557.
(5) Navýò, J. A.; Hidalgo, M. C.; Colón, G.; Botta, S. G.; Litter, M. I. *Langmuir* **2001**, *17*, 202−210.
(6) Shukla, S.; Seal, S.; Vij, R.; Bandyopadhyay, S.; Rahman, Z. *Nano Lett.* **2002**, *2*, 989−993.
(7) Noh, H. J.; Seo, D. S.; Kim, H.; Lee, J. K. *Mater. Lett.* **2003**, *57*, 2425−2431.
(8) Somîya, S.; Akiba, T. *J. Eur. Ceram. Soc.* **1999**, *19*, 81−87.
(9) Wu, J. M.; Wu, C. M. *J. Mater. Sci.* **1988**, *23*, 3290−3299.
(10) Zhang, Y. C.; Davison, S.; Brusasco, R.; Qian, Y. T.; Dwight, K.; Wold, A. *J. Less-Common Met.* **1986**, *116*, 301−306.
(11) Li, L. R.; Wang, W. Z. *Solid State Commun.* **2003**, *127*, 639−643.
(12) Woudenberg, F. C. M.; Sager, W. F. C.; Sibelt, N. G. M.; Verweij, H. *Adv. Mater.* **2001**, *13*, 514−516.
(13) Liang, J.; Deng, Z.; Jiang, X.; Li, F.; Li, Y. *Inorg. Chem.* **2002**, *41*, 3602−3604.
(14) Wang, X.; Zhuang, J.; Peng, Q.; Li, Y. D. *Nature* **2005**, *437*, 121−124.
(15) Pan, D. C.; Jiang, S. C.; An, L. J.; Jiang, B. Z. *Adv. Mater.* **2004**, *16*, 982−985.
(16) Wang, Q.; Pan, D. C.; Jiang, S. C.; Ji, X. L.; An, L. J.; Jiang, B. Z. *Chem.-Eur. J.* **2005**, *11*, 3843−3848.
(17) Pan, D. C.; Wang, Q.; Jiang, S. C.; Ji, X. L.; An, L. J. *Adv. Mater.* **2005**, *17*, 176−179.
(18) Pan, D.; Zhao, N.; Wang, Q.; Jiang, S.; Ji, X.; An, L. *Adv. Mater.* **2005**, *17*, 1991−1995.

10.1021/ja0612145 CCC: $33.50

The reaction occurred under a certain pressure at the interface between the two phases; this process probably facilitates the preparation of shape-controlled nanocrystals. (iv) The resulting nanocrystals were capped with alkyl chains, and thus they were soluble in nonpolar solvents.

Experimental Section

Materials. Oleic acid (OA, tech. grade, 90%) and myristic acid (MA, 99.5%) were purchased from Aldrich. Zirconium(IV) *n*-propoxide (25% in alcohol) was purchased from Strem Chemical Co. Decanoic acid (DA, 98%), dodecanoic acid (DDA, 98%), docosanoic acid (DCA), stearic acid (SA, 98%), and *tert*-butylamine (98.5%) were purchased from China Medicine Shanghai Chemical Reagent Corp.

Synthesis of ZrO_2 Nanocrystals. An aqueous solution (15 mL) of *tert*-butylamine (200−1000 μL) was loaded into a 30-mL Teflon-lined stainless steel autoclave. A toluene solution (5 mL) containing zirconium(IV) *n*-propoxide (150−900 μL), OA (1.0 mL), and SA (or MA, DA, DDA, or DCA; 0.5 g) was then transferred to the autoclave to provide a two-phase reaction system. Without stirring the mixture, the autoclave was sealed and maintained at 120−180 °C for a fixed period of time and cooled to ambient temperature using tap water. The crude solution of ZrO_2 nanocrystals was precipitated with methanol and further isolated by centrifugation and decantation. The purified nanocrystals were redispersed in organic solvents for optical and structural characterization without any size sorting.

Characterization of Nanocrystals. UV−vis absorption spectra were recorded on a Shimadzu UV-2450 double-beam recording spectrophotometer using 1-cm quartz cells. Fluorescence spectra were obtained on a Shimadzu RF-5301 instrument operated at a resolution of 1.0 nm. Transmission electron microscopy (TEM) images were obtained using a JEOL-1011 electron microscope operated at an accelerating voltage of 100 kV. Samples for TEM observation were prepared by dropping 10 μL of diluted toluene solution onto 400-mesh carbon-coated copper grids. The particle size and size distribution diagrams were obtained after careful measurement of more than 200 individual ZrO_2 nanoparticles. HRTEM measurements were performed using a JEOL-2010F transmission electron microscope operated at an acceleration voltage of 200 kV. X-ray powder diffraction (XRD) investigations were performed using a Rigaku D/MAX-2500 instrument (Cu Kα1 radiation) operated at 50 kV and 250 mA over the range 20−80° by step scanning with a step size of 0.02°. The crystallite sizes were estimated using Scherrer's method. Raman spectra were recorded at room temperature using a FT-Raman 960 instrument equipped with a 1064-nm laser beam. XRD and Raman samples were prepared through the evaporation of one drop of concentrated nanocrystal solution that had been placed on a glass plate.

Results and Discussion

(1) Effect of Reaction Time. The TEM images in Figure 1 indicate that the shapes of the nanocrystals could be tuned through control of the reaction time. At the beginning of the reaction, the formation of nuclei was predominant. If the chemically stable precursors produced a small number of nuclei, we would expect the nanocrystals to grow into an elongated shape if the monomer concentration remained relatively high after nucleation.[19] After a reaction time of 12 h, we obtained roughly spherical particles having an average diameter of 2.9 nm (Figure 1a); the corresponding HRTEM image of an isolated 3.7 nm ZrO_2 nanoparticle is presented in Figure 1e. The clear lattice image indicates the high crystallinity of the as-synthesized nanoparticles. We clearly observe a lattice spacing of 0.318 nm

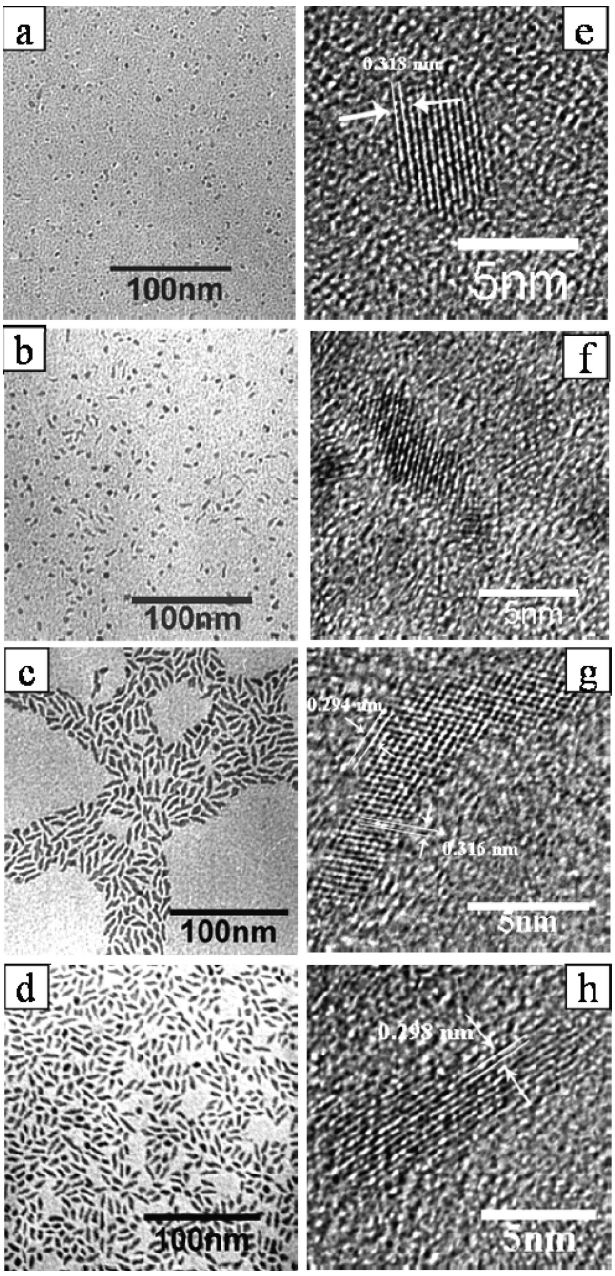

Figure 1. (a−d) TEM images of ZrO_2 nanocrystals prepared at 180 °C and a monomer concentration [Zr] of 0.2 M for different reaction times: (a) 12, (b) 24, (c) 72, and (d) 120 h. (e−h) HRTEM images obtained after reaction times of (e) 12, (f) 24, (g) 72, and (h) 120 h.

for the $(\bar{1}11)$ plane of the monoclinic ZrO_2 structure. Zirconium(IV) *n*-propoxide is a relatively inactive precursor because of the presence of its inert *n*-propoxide groups; thus, the system produces a relatively small number of nuclei. When the monomer concentration decreases to a critical value, these nuclei will consume the remaining monomers and the nanocrystals tend to form elongated shapes.[19−21] It appears that the particle growth occurred selectively on one face of the rods such that almost teardrop-shaped particles formed with minimal surface energy (Figure 1b). The teardrop-shaped particles, which had an average length of ca. 8.6 nm, amounted to no less than 36% in the sample. Figure 1f presents a HRTEM image of an isolated

(19) Peng, X. G.; Wickham, J.; Alivisatos, A. P. *J. Am. Chem. Soc.* **1998**, *120*, 5343−5344.
(20) Peng, Z. A.; Peng, X. G. *J. Am. Chem. Chem.* **2001**, *123*, 183−184.
(21) Peng, Z. A.; Peng, X. *J. Am. Chem. Soc.* **2002**, *124*, 3343−3353.

Table 1. The Volume Fraction of Monoclinic Phase at Different Reaction Time

reaction time	X_m	V_m
12 h	0.103	0.131
24 h	0.454	0.522
48 h	0.476	0.544
72 h	0.572	0.637
5 days	0.555	0.621
7 days	0.580	0.644

teardrop-shaped ZrO_2 nanoparticle. Manna et al.[22] were the first to observe this shape during the synthesis of CdSe nanocrystals; they considered that it resulted from an Ostwald ripening process occurring at very low monomer concentrations, followed by a rapid increase in the monomer concentration upon further injection. Peng[21,23] also observed tadpole-like CdSe nanorods whose morphologies were similar to the teardrop-like nanocrystals mentioned above. They suggested that rods of a certain length grew into tadpole-shapes because of asymmetric growth along the *c*-axis. Obviously, this explanation is not valid for our samples because of the different reaction conditions that we employed. It may be possible that, in our system, a dot formed the body of a tear and then the droplet elongated along only one facet during the growth process. A further increased reaction time resulted in an increase in the lengths of the clusters as a result of growth along the thin end. It was also possible for two rods to become linked in a head-to-head manner to form a new "hump-back" rod rather than a straight rod (Figure 1c). The corresponding HRTEM image in Figure 1g is that of a nanoparticle having a length of 16.0 nm and an aspect ratio of 6. The distances between the two adjacent planes are 0.294 nm (top) and 0.316 nm (bottom), corresponding to the (111) and ($\bar{1}$11) planes in tetragonal and monoclinic ZrO_2 phases. Up to a certain time, the rods gradually became relatively smoother and their sizes decreased slightly. For example, the average particle length in Figure 1d is 12.8 nm. The representative HRTEM image in Figure 1h is that of an isolated ZrO_2 nanoparticle having a length of 12.6 nm and an aspect ratio of 3. The distance between the two adjacent planes is 0.298 nm, which corresponds to the (111) planes of the tetragonal phase of ZrO_2. At this stage, the remaining monomer concentration in the system was lower than the solubility of the as-prepared clusters, and thus the clusters dissolved. To minimize the surface energy of a given nanocrystal, atoms from relatively higher surface energy positions relocated to the lower-energy sites; this process led to the formation of nanocrystals having relatively smooth surfaces.[21]

The volume fraction of monoclinic phase was summarized in Table 1. It was calculated by the following equations.[7]

$$V_m = 1.311X_m/(1 + 0.311X_m) \quad (1)$$

$$X_m = [I_m(111) + I_m(\bar{1}11)]/[I_t(111) + I_m(\bar{1}11) + I_m(111)] \quad (2)$$

where V_m is the volume fraction of monoclinic phase, X_m is the integrated intensity ratio, $I_m(111)$ is the (111) intensity of monoclinic ZrO_2, $I_m(\bar{1}11)$ is the ($\bar{1}$11) intensity of monoclinic ZrO_2, and $I_t(111)$ is the (111) intensity of tetragonal ZrO_2.

ZrO_2 exists in three polymorphs: the monoclinic, tetragonal, and cubic phases. Normally, the monoclinic phase is thermodynamically stable at room temperature, while the tetragonal and cubic phases exist only at high temperature above 1170 and 2380 °C, respectively.[11] These two high-temperature phases are unstable in bulk forms at ambient temperature, but Garvie[24] predicted that pure ZrO_2 is stabilized in the tetragonal form at room temperature when the (spherical) particle size is less than 30 nm. As far as our system is concerned, the size of the obtained particle is in the range of critical size predicted in the literature. If it obeys the surface-energy theory, the tetragonal polymorph should be spontaneous stabilization in pure zirconia. However, upon increasing the reaction time, the fraction of monoclinic phase increased from 0.137 to 0.644 (Figure 2, Table 1). The occurrence of mixed phase indicates that the stability of metastable phase cannot be explained adequately by the surface-energy theory.

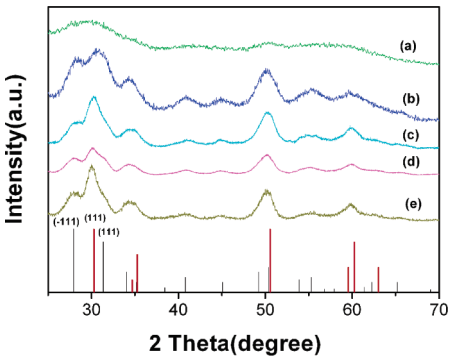

Figure 2. Temporal evolution of XRD patterns of OA-capped ZrO_2 nanocrystals: (a) 12, (b) 24, (c) 48, (d) 72, and (e) 120 h. The bulk crystalline ZrO_2 diffraction lines are indicated as vertical bars; the thinner and thicker lines represent monoclinic and tetragonal structures, respectively.

The correlated changes in shape and phase of ZrO_2 particles have been mentioned in the literature. Nishizawa et al.[25] reported that amorphous ZrO_2 transforms into the crystalline form at 130 °C under hydrothermal treatment; however, at a reaction temperature of 320 °C, the cubic crystallites abruptly transform to needlelike monoclinic ZrO_2. They suspected that the smaller particles migrate and align themselves to form the larger monoclinic rods. Noh et al.[7] reported that ZrO_2 nanocrystals with anisotropic shapes and various crystal structures were synthesized by a hydrothermal process. The spherical particles with a tetragonal phase were changed into the long rodlike particles with a monoclinic phase with increasing reaction temperature. They speculate that the monoclinic rods form through the dissolution and reprecipitation, or by coagulation of very fine particles in a highly oriented fashion. Recently, Brus et al.[26,27] reported that roughly spherical particles with tetragonal phase form, whereas at higher temperatures (400 °C), the particles form as nanorods; meanwhile, the tetragonal phase changes to the monoclinic phase. The authors confirm that this concomitant phase and shape change is a result of martensitic transformation of isolated nanocrystals in a hot liquid.

At present, we believed that the nuclei (the coexistence of monoclinic and tetragonal) could form as a result of the

(22) Manna, L.; Scher, E. C.; Alivisatos, A. P. *J. Am. Chem. Soc.* **2000**, *122*, 12700−12706.
(23) Peng, X. *Adv. Mater.* **2003**, *15*, 459−463.
(24) Garvie, R. C. *J. Phys. Chem.* **1978**, *82*, 218−224.
(25) Nishizawa, H.; Yamasaki, N.; Matsuoka, K.; Mitsushio, H. *J. Am. Ceram. Soc.* **1982**, *65*, 343−346.
(26) Tang, J.; Fabbri, J.; Robinson, R. D.; Zhu, Y.; Herman, I. P.; Steigerwald, M. L.; Brus, L. E. *Chem. Mater.* **2004**, *16*, 1336−1342.
(27) Tang, J.; Zhang, F.; Zoogman, P.; Fabbri, J.; Chan, S. W.; Zhu, Y.; Brus, L. E. *Adv. Funct. Mater.* **2005**, *15*, 1595−1602.

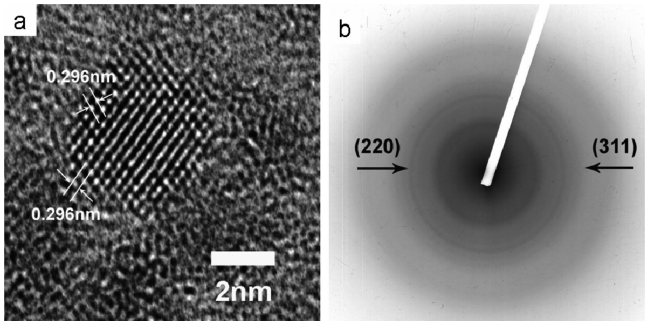

Figure 3. (a) High-resolution TEM (HRTEM) image of one OA-capped ZrO_2 nanocrystal for 4 h. (b) Selected area electron diffraction pattern of sample in (a).

martensitic transformation and then subsequently come into the growth stage, which is controlled by the diffusion mechanism, based on the following evidence.

(i) We have obtained considerable structure information from high-resolution TEM (HRTEM) for the relatively smaller nanoparticle. Figure S1 shows the high-resolution TEM (HRTEM) image of OA-capped zirconia nanocrystal at the earliest stage (reaction time is 2 h in the Supporting Information). The typical HRTEM image in the inset is that of an isolated ZrO_2 nanoparticle having a diameter of 2.8 nm. We clearly observe a lattice spacing of 0.294 nm for the (111) plane of the tetragonal ZrO_2 structure. Figure 3a shows the HRTEM image of an isolated 3.6 nm ZrO_2 nanoparticle for 4 h. The clear lattice image indicates the high crystallinity and single crystalline nature of ZrO_2. The lattice spacing of 0.296 nm for the (111) planes of the tetragonal structure can be readily resolved. Figure 3b is the selected area electron diffraction (SAED) pattern acquired from the ZrO_2 sample for 4 h. The detectable rings are indexed to the same position as those from standard tetragonal ZrO_2 (JCPDS File No. 14-0534). At the earliest stage, the ZrO_2 nanocrystals are the pure or predominantly tetragonal phase form. After a reaction time of 12 h, the size of as-prepared nanocrystals slightly increases as compared to the nuclei, but the structure changed a lot. Further structure information can be obtained using the XRD patterns (Figure 2a). It indicates that the obtained nanocrystals exist with a mixture of monoclinic and tetragonal phases. Confessedly, martensitic transformation is diffusionless and accompanied by a little change in volume. Thereby, we supposed the martensitic transformation occurred in the initial stages.

(ii) Figure 2 indicates that the as-prepared samples are polymorphs. In addition, the monoclinic and tetragonal coexisted in one particle (such as Figure 1g) and did not exist beneath each other in different particles. As far as we know, the coexistence of both polymorphs in one particle is an indication for the martensitic transition character.[28]

(iii) Both high-resolution TEM images and X-ray diffraction investigations show that twinning structures occur in the monoclinic nanocrystals. The details will be discussed in the section of the effect of capping agent. Generally, twinning is a typical result of martensitic phase transformation. Therefore, the twinning structures observed provide very important evidence for the phase changes of the nuclei resulting from the martensitic phase transformation.

(iv) The percentage of the monoclinic phase increases with increased reaction time. (cf., Figure 2b−e). However, in the terminal stage, we cannot obtain the pure monoclinic ZrO_2; the fraction of the monoclinic phase did not show the significant increment. In the martensitic transformation, a larger driving force may be needed for ZrO_2 than for HfO_2, etc.[27] Brus et al. reported they only observed the t→m transformation for HfO_2 and Hf-rich $Hf_xZr_{1-x}O_2$ nanoparticle. Hence, the incomplete t→m transformation resulting in the tetragonal phase remained. In addition, the martensitic transformation is independent of time at a fixed temperature and only changes by varying the temperature.

In summary, an explanation based on the concept of a martensitic transformation in the initial stages may be more reasonable. It is clear that the shapes of the nanocrystals could be controlled very well merely by adjusting the reaction time for the subsequent growth. The shape change is the result of both the martensitic transformation and the diffusion mechanism, which more effect the nucleation and growth, respectively.

(2) Effect of Capping Agent. The nature of the capping agent also played an important role in controlling the shapes of the nanocrystals. Figures 4a−d and 1c indicate that we could obtain branched structures, that is, leaf-, arrow-, rice-, rod-, and dot-shaped nanocrystals, when using the same or different capping agents. The HRTEM images in Figures 4f−i and 1g reveal structure information about these nanocrystals and also indicate the respective distances between their two adjacent planes. Figure 4j displays the selected area electron diffraction (SAED) pattern acquired from the corresponding DCA-capped ZrO_2 nanoparticles. All of the detectable rings are indexed perfectly to the same positions as those of standard tetragonal-phase ZrO_2. This result implies that the fraction of monoclinic phase was very low. It is known that the presence of differently shaped II−VI semiconductor nanocrystals can be attributed to the fact that they are formed through a diffusion-controlled growth process. During diffusion-controlled crystal growth, a diffusion sphere surrounds each crystal. The monomer concentration gradient between the bulk solution and the stagnant solution, as well as the diffusion coefficient of the monomers, determines the direction (out or into the diffusion sphere) of growth and the diffusion flux. The monomer concentration in the stagnant solution maintains the solubility of a given facet through rapid growth onto or dissolution away from the facet.[29] A longer hydrocarbon chain results in a slower reaction rate because of the smaller diffusion coefficient. When we increased the length of the hydrocarbon chain of the capping agents from C_{10} to C_{22} (DA < DDA < MA < SA < DCA), we found that the shapes of the nanocrystals tended to vary from branched to spherical structures; this result is in good agreement with the diffusion mechanism described above. The XRD patterns in Figure 5 imply that the fraction of the monoclinic phase decreased upon increasing the length of the hydrocarbon chain (see Table 2); this finding may be consistent with martensitic transformation. Brus et al. considered the martensitic transformation kinetics are controlled by nucleation and growth; in nature, these transformation are nucleation-controlled. They believed that the t→m transformation of nanoparticle is facilitated in the surfactant (trioctylphosphine oxide, TOPO), and this is probably due to the enhancement of the nucleation in the presence of surfac-

(28) Nitsche, R.; Rodewald, M.; Skandan, G.; Fuess, H.; Hahn, H. *Nanostruct. Mater.* **1996**, *7*, 535−546.

(29) Peng, Z. A.; Peng, X. G. *J. Am. Chem. Soc.* **2001**, *123*, 1389−1395.

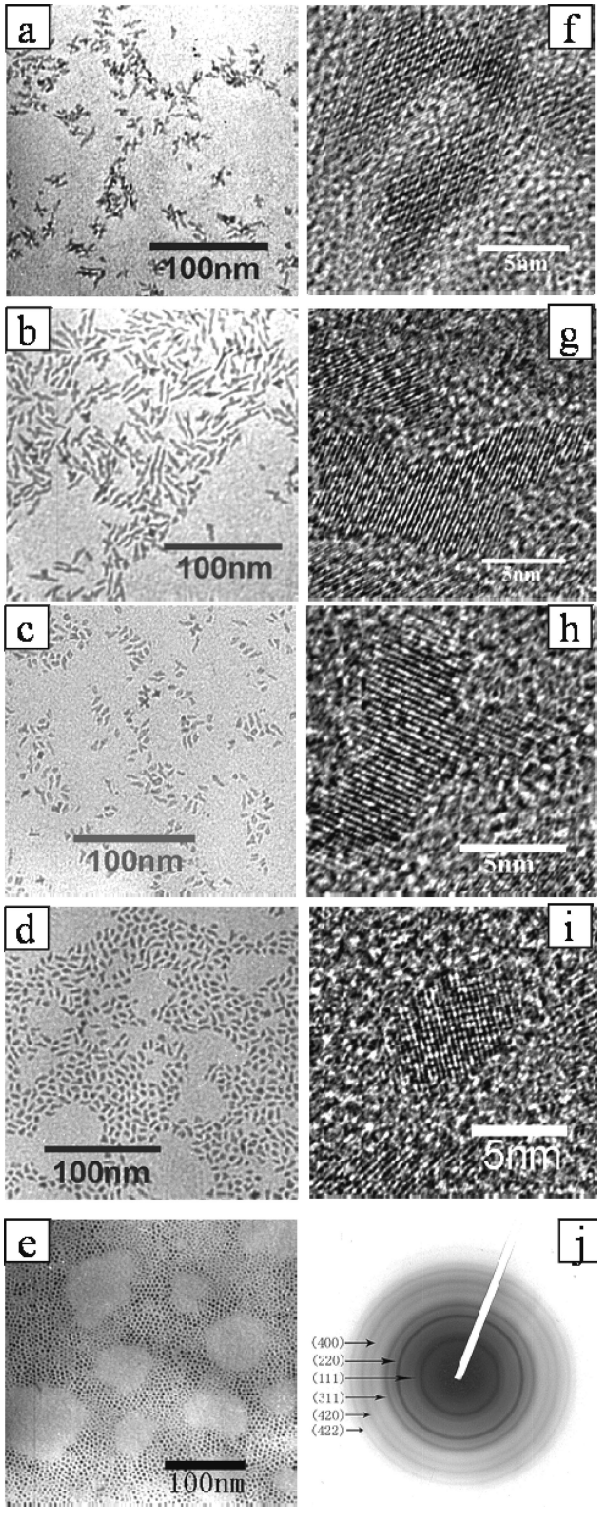

Figure 4. (a−e) TEM images of ZrO_2 nanocrystals prepared at a monomer concentration [Zr] of 0.2 M for 72 h in the presence of different capping agents: (a) DA, (b) DDA, (c) MA, (d) SA, and (e) DCA. (f−i) Corresponding HRTEM images: (f) DA, (g) DDA, (h) MA, and (i) SA. (j) Selected area electron diffraction pattern of the DCA-capped ZrO_2 nanocrystal.

tants.[27] For instance, the DDA-capped ZrO_2 nanocrystals are the pure monoclinic phase form and the DCA-capped ZrO_2 nanocrystals are predominantly the tetragonal phase form. A longer hydrocarbon chain results in a slower nucleation and confines the martensitic phase transformation to some extent. Brus and co-workers found the twinning structures in the

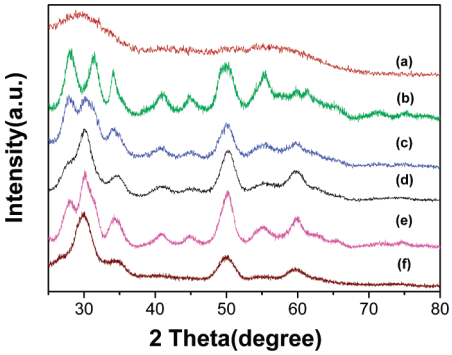

Figure 5. XRD patterns of ZrO_2 nanocrystals prepared at monomer concentration [Zr] = 0.2 M for 72 h in the presence of different capping agents: (a) DA, (b) DDA, (c) MA, (d) SA, (e) OA, and (f) DCA.

Table 2. The Volume Fraction of Monoclinic Phase with Different Capping Agent

capping agent	X_m	V_m
DDA	1.000	1.000
MA	0.585	0.649
SA	0.333	0.392
DCA	0.083	0.106

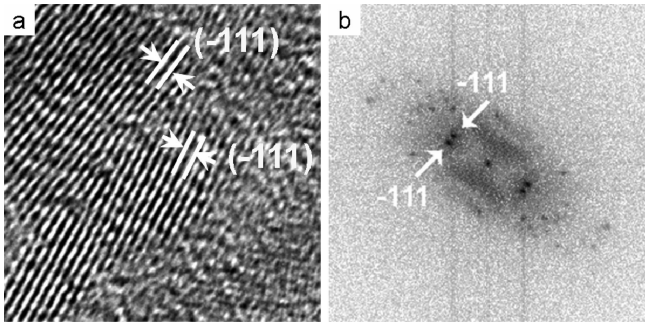

Figure 6. (a) HRTEM image of DDA-capped ZrO_2 nanocrystals. (b) The corresponding diffraction pattern obtained from Fourier transforming the image in (a).

monoclinic nanorods. Similarly, we observed the analogous structure in the sample of DDA-capped ZrO_2 nanocrystals. The representative HRTEM image in Figure 6a is that of monoclinic nanocrystals, in which the twinning element is clearly identified. Figure 6b is a Fourier transformation of the corresponding HRTEM image, and the twinning is further confirmed by spot splitting in the diffraction pattern. Definitely, the martensitic phase transformation exists in our system.

We also obtained considerable structure information from the Raman spectra. Figure 7 presents the reduced Raman spectra of the OA- and DDA-capped ZrO_2 samples after their annealing at 400 °C for 1 h to remove the organic ligands. As compared to the spectrum of bulk monoclinic ZrO_2,[30] we attribute the two strong peaks at 148 and 270 cm^{-1} to the tetragonal phase. Measured with one of the modes, the peak at 478 cm^{-1} is present in both monoclinic and tetragonal phases. These results suggest that a mixture of monoclinic and tetragonal phases coexists, which is in good accordance with our XRD data.

Figure 8 displays the UV−vis absorption and photoluminescence (PL) spectra of the DA-capped ZrO_2 nanocrystals in toluene. Figure 8a indicates that a clear absorption onset occurs at ca. 3.2 eV. Figure 8b displays the PL spectrum obtained using

(30) Keramidas, V. G.; White, W. B. *J. Am. Ceram. Soc.* **1974**, *57*, 22−24.

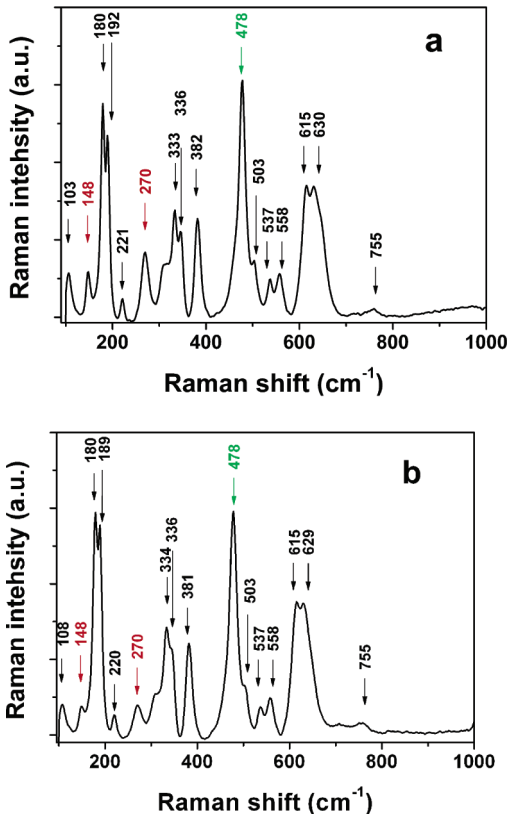

Figure 7. Raman scattering spectra of ZrO_2 nanocrystals prepared using (a) OA and (b) DDA as capping agents.

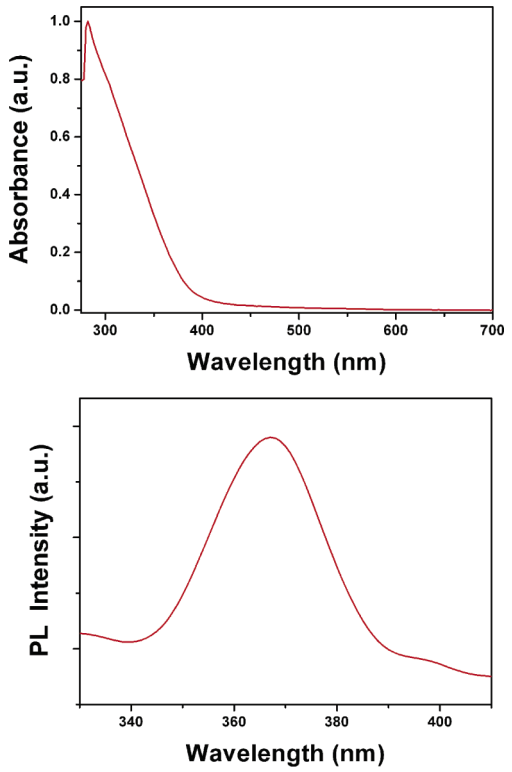

Figure 8. (Top) UV−vis absorption and (bottom) PL spectra of DA-capped ZrO_2 nanocrystals.

an excitation wavelength of 250 nm; the emission was centered at ca. 365 nm. These features are probably related to the involvement of a mid-gap trap state that results from incomplete surface passivation.

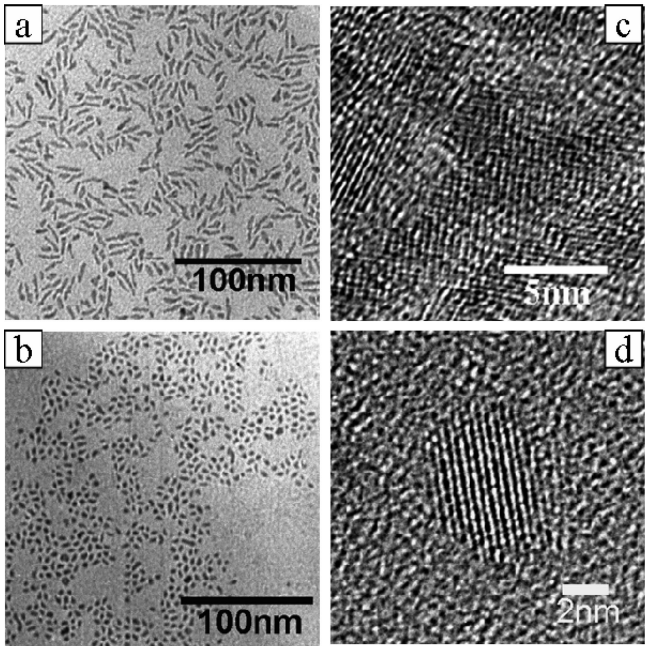

Figure 9. (a,b) TEM images of ZrO_2 nanocrystals prepared over 72 h at [Zr] monomer concentrations of (a) 0.07 M and (b) 0.4 M. (c,d) Corresponding HRTEM images: (c) [Zr] = 0.07 M, (d) [Zr] = 0.4 M.

(3) Effect of Monomer Concentration. The monomer concentration is also a key factor in controlling the shape. At a high monomer concentration, we observed rice-like nanocrystals having an average length of 5.1 nm (Figure 9b). The typical HRTEM image in Figure 9d is that of an isolated ZrO_2 nanoparticle having a length of 7.2 nm. We readily resolve a lattice spacing of 0.317 nm for the $(\bar{1}11)$ planes of the monoclinic ZrO_2 structure. During the initial stages of the synthetic procedure, the system produced a relatively large number of nuclei because of the high monomer concentration. As a result, the amount of monomer remaining for growth was relatively low. When the monomers entering the diffusion sphere are shared for growth in all three dimensions,[21] the particles gradually form into shapes resembling rice grains. When the monomer concentration was relatively low, these nuclei consumed the remaining monomers and the nanocrystals tended to form with elongated shapes. The roughly rod-shaped nanocrystals exhibited in Figures 9a and 1d possessed average lengths of 15.5 and 14.5 nm, respectively.

In general, the nucleation process is a crucial step for the formation of the rod-shaped and other elongated structures. A relatively high monomer concentration is required during the formation of the elongated shapes. An excessively high monomer concentration, however, did not lead to the appearance of elongated shapes because of the rapid nucleation process.

(4) Effect of Reaction Temperature. The reaction temperature also influences the shapes of nanocrystals. Figure 10 displays TEM images of the nanocrystals produced after typical syntheses at different temperatures, but with a fixed reaction time (72 h). The nanocrystals prepared at 120 and 150 °C exhibit roughly spherical shapes, similar to those in Figure 1a and b, whereas the samples obtained at 180 °C possessed branched structures. In addition, the percentage of the monoclinic phase is decreased at lower temperature (the volume fraction of monoclinic phase was 0.327). In fact, the interplay of chemical and mechanical (stain) forces plays an important role on the

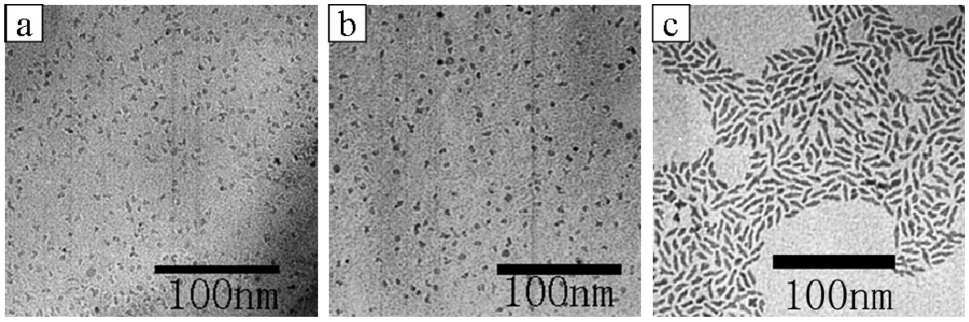

Figure 10. TEM images of ZrO_2 nanocrystals prepared for 72 h at [Zr] = 0.2 M at reaction temperatures of (a) 120, (b) 150, and (c) 180 °C.

reaction process stepwise over a range of temperatures.[31] The martensitic transformation is conspicuous by their predominantly athermal character, meaning that the phase transformation keeps pace with the temperature and independent of the time at a fixed temperature.[27,31] In the first instance, it is much more difficult to transform with the lack of driving force and the significantly decreased transformation rate at low temperature. At the growth stage, some small particles are unable to grow into large ones due to a lower probability of their arrival at the interface from the oil phase. It seems that a lower temperature can lead to incomplete mixing between the aqueous phase and organic phase and a lower degree of monomer diffusion when compared to those reacted at higher temperatures. Apparently, it is unfavorable for nucleation, phase transformation, and growth at low temperature. However, a high reaction temperature readily facilitates control over the shape of nanocrystals only through varying the reaction time.

Conclusions

We have applied a two-phase approach to the successful synthesis of colloidal zirconia nanocrystals having different morphologies, including spherical-, teardrop-, rod-, and rice-shaped particles. The shape change is the result of both the martensitic transformation and the diffusion mechanism, which more effect the nucleation and growth, respectively. It is clear that the shapes of the nanocrystals could be controlled very well merely by adjusting the reaction time, the nature of the capping agent, the monomer concentration, and the reaction temperature for the subsequent growth. TEM images suggested that the shapes of these nanocrystals varied from branched structures to spheres upon increasing the length of the hydrocarbon chain of the capping agent due to a slower nucleation and confining the martensitic phase transformation to some extent at the initial stage. The XRD patterns and Raman spectra indicate that the as-prepared particles existed as mixtures of monoclinic and tetragonal phases. A fluorescence spectrum recorded after excitation at 250 nm displayed a broad band at ca. 365 nm. We believe that the nanocrystals possessing anisotropic shapes, for example, the rod- and rice-shaped particles, might find applications in films, ceramic coatings, and related devices. Indeed, we hope that this simple, reproducible, and low-cost method will be exploited in the future for large-scale syntheses of zirconia and other metal oxides nanocrystals.

Acknowledgment. We are grateful for the support for this study provided by the National Natural Science Foundation of China (90101001, 50073024), the Distinguished Young Fund of Jilin Province (20050104), the Chinese Academy of Sciences (project KJCX2-SW-H07), and the International Collaboration Project (04-03GH268, 20050702-2) from Changchun City and Jilin Province, China. X.J. thanks Dr. L. An's group for assistance in obtaining the UV and PL spectra. N.Z. thanks Dr. L. Sun and Dr. R. Xie for their help in analysis of structure information.

Supporting Information Available: High-resolution TEM (HRTEM) image of OA-capped zirconia nanocrystal (Figure S1). This material is available free of charge via the Internet at http://pubs.acs.org.

JA0612145

(31) Wolten, G. M. *J. Am. Ceram. Soc.* **1963**, *46*, 418−422.